

Supporting Information

Intermeshing Electron Transporting Layer for Efficient and Stable CsPbI₂Br Perovskite Solar Cells with Open Circuit Voltage over 1.3 V

Shuo Liu,^a Weijie Chen,^a Yunxiu Shen,^a Shuhui Wang,^a Moyao Zhang,^a Yaowen Li,*^a Yongfang Li^{a,b}

^a Laboratory of Advanced Optoelectronic Materials, College of Chemistry, Chemical Engineering and Materials Science, Soochow University, Suzhou 215123, China

^b Beijing National Laboratory for Molecular Sciences; Institute of Chemistry, Chinese Academy of Sciences, Beijing 100190, China

*Corresponding Author: Email: ywli@suda.edu.cn (Li. Y. W.)

Keywords: intermeshing SnO₂; antireflection; energy loss; cascade energy level; inorganic perovskite solar cells

Experimental Section

Materials:

ITO glass was purchased from South China Xiang Science and Technology Company, Ltd.. The SnO₂ colloid precursor was purchased from Alfa Aesar (tin (IV) oxide, 15 wt% in H₂O colloidal dispersion). The SnCl₂·2H₂O and 4-tert-butylpyridine (tBP) were purchased from ALDRICH. PbI₂ (Lead (II) iodide, 99.999%) was purchased from Alfa Aesar. CsI (Cesium Iodide, 99.99%), PbBr₂ (Lead (II) Bromide, 99.99%), Spiro-OMeTAD (2,2,7',7'-tetrakis(N,N-di-4-methoxyphenylamine)-9,9'-spirobifluorene, 99.8%) and Bis(trifluoromethylsulfonyl)amine lithium salt (Li-TFSI) were purchased from Xi'an Polymer Light Technology Corp. Dimethyl sulfoxide (DMSO, ultradry) was purchased from J&K. Chlorobenzene (CB, 99.8%) was purchased from sigma-ALDRICH. All the materials were used as received without any purification.

Fabrication of NP-SnO₂, Col-SnO₂ and Im-SnO₂ films:

ITO glass substrates were sequentially washed with isopropanol, acetone, distilled water, and ethanol for 20 minutes, respectively, and then dried in an oven. ITO glass substrates were treated with UV ozone for 20 minutes before spin-coating ETL.

NP-SnO₂ ETL: The SnO₂ precursor was obtained by dissolving 22.6 mg SnCl₂·2H₂O in 1 mL ethanol. The solution was stirred for 1 h, subsequently filtered the solution with a 0.45-μm PTFE membrane. Before coating NP-SnO₂ solution, the UVO-treated ITO substrate is pre-heated at 50 °C for 2 minutes to avoid the fogging of NP-SnO₂ film, then the NP-SnO₂ films were fabricated by spin-coating the above solution onto the ITO substrates at 4000 rpm for 30 s, followed by thermal annealing on a hot plate at 150 °C for 30 min in ambient atmosphere.

Col-SnO₂ ETL: The SnO₂ colloid precursor (171 mg/mL) was diluted to 28 mg/mL with deionized water, then the solution was stirred for 1 h at room temperature. The Col-SnO₂ films were obtained by spin-coating the above solution onto the ITO substrates at 2000 rpm for 30 s, followed by thermal annealing on a hot plate at 150 °C for 30 min at ambient atmosphere.

Im-SnO₂ ETL: The prepared NP-SnO₂ film was treated with UV ozone for 10 minutes to improve the penetration/contact of Col-SnO₂ solution, then Im-SnO₂ films were obtained by spin-coating Col-SnO₂ precursor solution on the UV ozone treated NP-SnO₂ films at 6000 rpm for 30 s, followed by thermal annealing in ambient atmosphere. We firstly optimized the thickness of Col-SnO₂ layer in Im-SnO₂ ETL to realize the highest charge carrier extracting efficiency, the film thickness is tuned by changing the spin-coating speeds, and it was found that the champion efficiency is achieved by spin-coating NP-SnO₂ at a spin-coating speed of 4000 rpm and Col-SnO₂ at 6000

rpm. The same fabrication parameters were used to spin-coat these SnO₂ ETLs on the silicon substrate to measure their reflection index and compare their thickness by using an ellipsometer.

Device Fabrication:

After depositing ETL on the cleaned ITO substrates, the samples were transferred into a nitrogen-filled glovebox. The CsPbI₂Br precursor solution was prepared by dissolving stoichiometric-ratio CsI, PbBr₂, and PbI₂ in DMSO with a 1.2 M solution. Before using it, the solution was stirred at 70 °C for 6 h and then filtered by a 0.45-μm PTFE membrane. After that, the CsPbI₂Br perovskite films were deposited by spin-coating CsPbI₂Br precursor on SnO₂ ETL at 3000 rpm for 30 s, subsequently the film was treated with a gradient thermal annealing process 1) 50 °C for 1 minute; 2) 100 °C for 1 minute; 3) 160 °C for 10 minutes. As for the hole transporting layer (HTL), Spiro-OMeTAD in chlorobenzene with a concentration of 80 mg/mL was blended with 17.5 mL of lithium bis(trifluoromethanesulfonyl)imide in acetonitrile (520 mg/mL) and 30 mL of 4-tert-butylpyridine, then the mixture was coated onto the CsPbI₂Br film at 4000 rpm for 30 s. Finally, the counter electrode was deposited by thermal evaporation of 60-nm-thick gold under a pressure of 4×10⁻⁵ MPa. The active area is 0.1 cm².

Characterization:

The transmittance, absorption and reflection spectra were measured with ultraviolet spectrometer (Agilent Technologies Cary 5000 UV-Vis-NIR). SEM images were collected on a SU8010 produced by Hitachi, where the electron beam was accelerated at 5 kV. XRD patterns were collected using X'Pert Pro MPD (PANalytical B.V.). Photoluminescence (PL) was tested by a FLS980 (Edinburgh Instrument, UK), and transient photoluminescence measurements also used the FLS980 (Edinburgh Instrument, UK). The J-V characteristics of the devices were measured of under an illumination of AM 1.5G (100 mW/cm²) using a SS-F5-3A solar simulator (AAA grade, 50 × 50 mm² photobeam size) of Enli Technology Co., Ltd., the light intensity was corrected by a standard silicon solar cell. EQE spectrum was obtained by a solar cell spectral response measurement system (Enli Technology Co., Ltd., QE-R3011). C²-V spectra were measured with a Zahner Ennium Electrochemical Workstation. UPS was tested by a Kratos Axis Ultra DLD. The frequency-modulation (FM) KPFM was operated combined with a Cypher S AFM (Asylum Research, Oxford Instruments) and a HF2LI Lock-in amplifier (Zurich Instruments). The UV irradiation was provided by UV resource (PORTA-RAY 400R) with an intensity of 100 mW/cm² and wavelength of 365 nm. The UV irradiation stability test was performed in a glove box with an air conditioner for cooling samples.

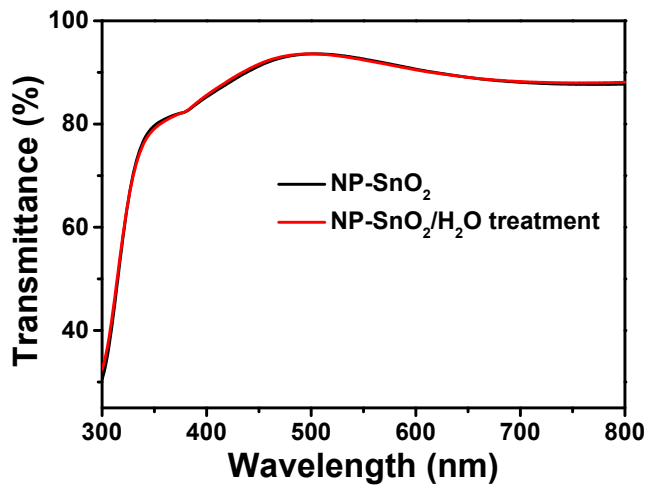


Figure S1. Transmittance spectra of NP-SnO₂ films before and after washing with H₂O.

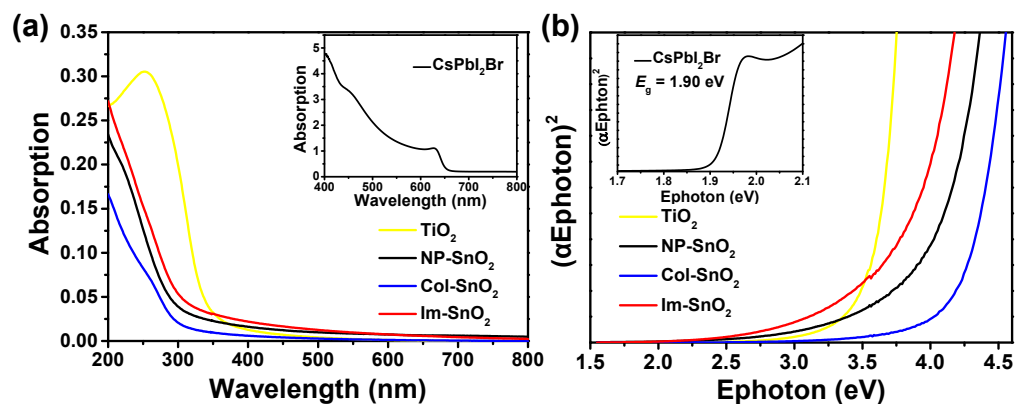


Figure S2. a) UV-vis absorption spectra and b) Tauc plots of SnO₂, TiO₂ and CsPbI₂Br perovskite films.

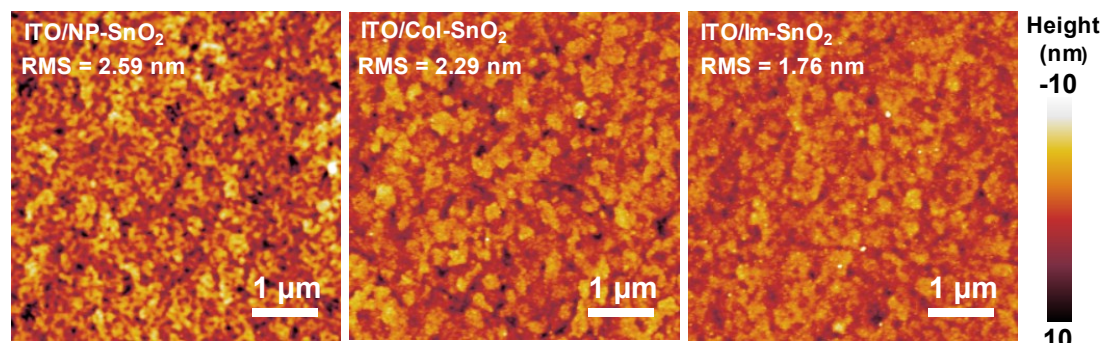


Figure S3. Atomic force microscopy (AFM) images of different SnO₂ ETLs deposited on ITO substrate.

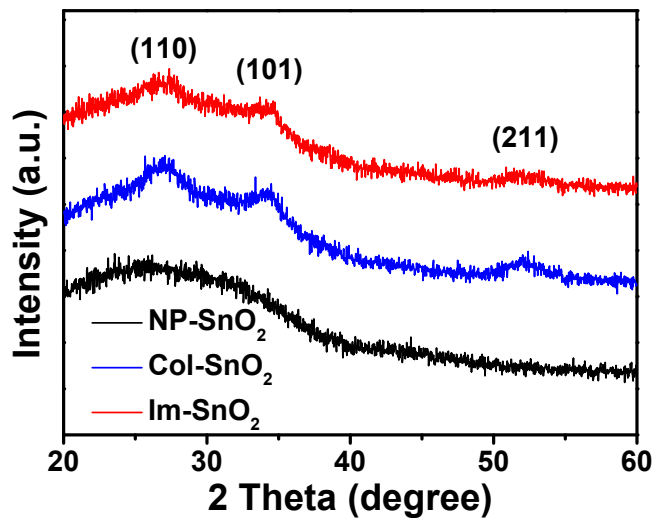


Figure S4. XRD patterns of NP-SnO₂, Col-SnO₂, and Im-SnO₂ films.

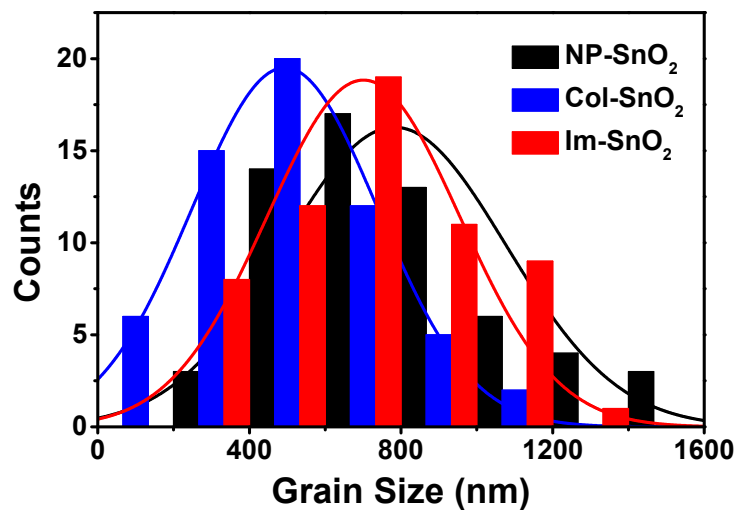


Figure S5. Grain size distribution of the perovskite films grown on different SnO₂ ETLs.

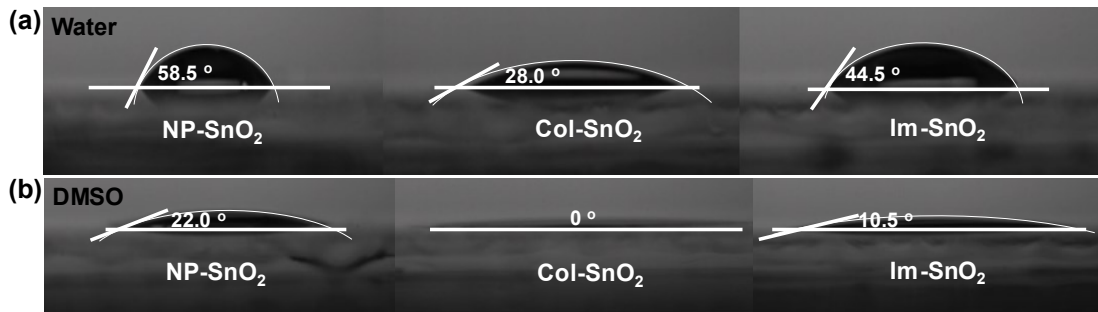


Figure S6. The images of the a) Water contact angles, b) DMSO contact angles on the NP-SnO₂, Col-SnO₂ and Im-SnO₂ ETLs.

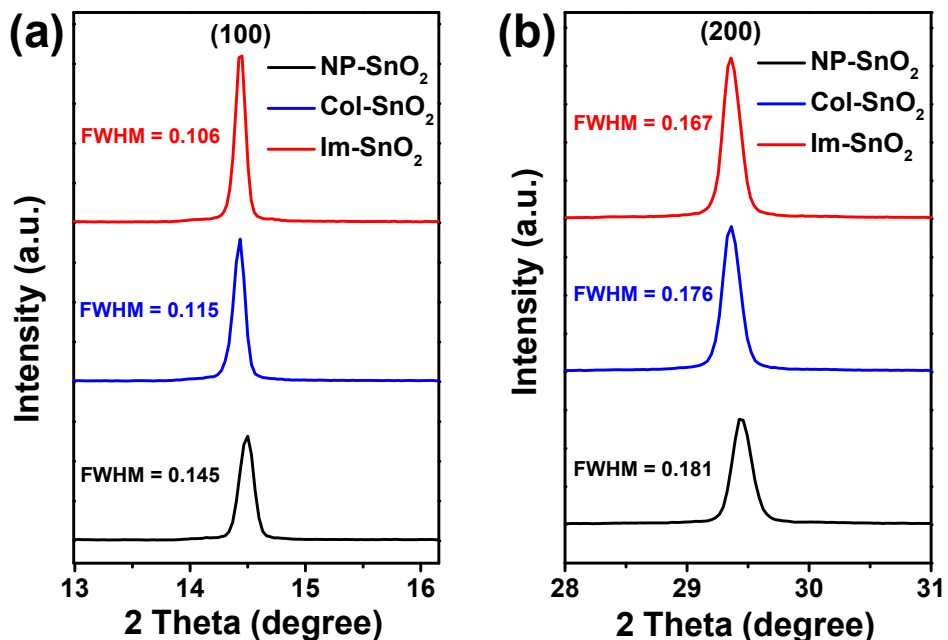


Figure S7. The zoomed-in regions of (100) and (200) diffraction peaks for CsPbI₂Br films deposited on different ETLs.

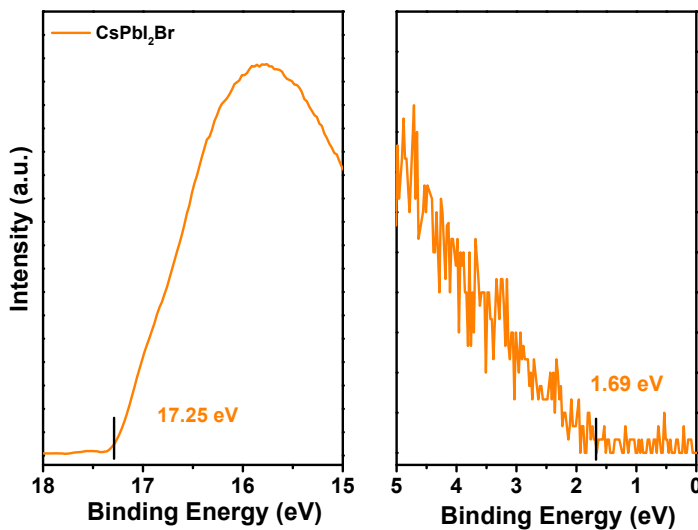


Figure S8. UPS spectrum of CsPbI₂Br film.

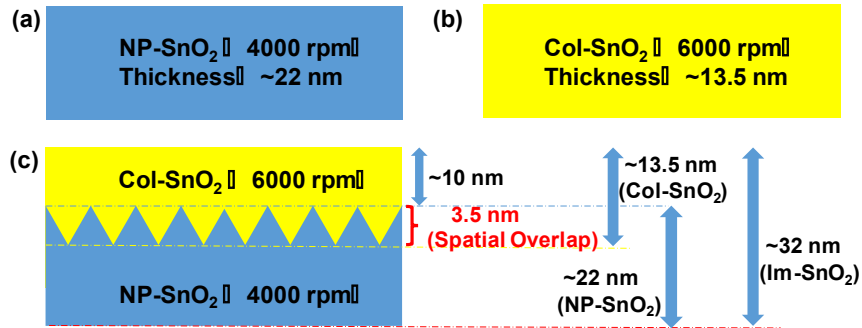


Figure S9. Thickness of a) NP-SnO₂ film at the spin-coating speed of 4000 rpm and b) NP-SnO₂ film at the spin-coating speed of 6000 rpm. c) The distribution diagram of NP-SnO₂ and Col-SnO₂ thickness in Im-SnO₂.

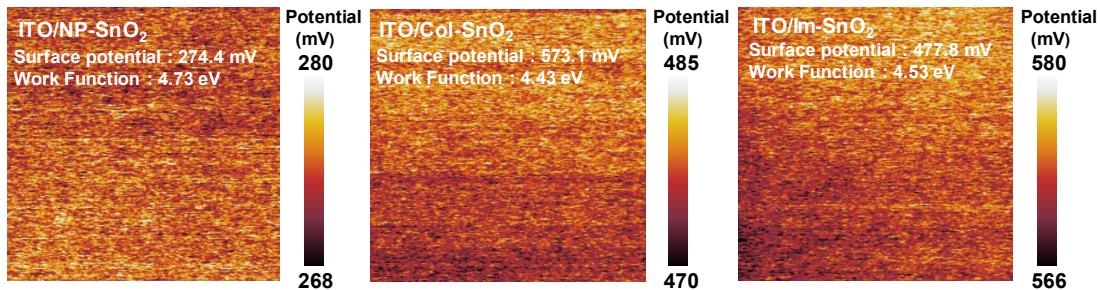


Figure S10. Surface potential images of NP-SnO₂, Col-SnO₂ and Im-SnO₂ films. Their surface potentials were measured by probing the contact potential difference (CPD) between the tip and the samples. Then the corresponding work function was calculated according to the equation:

$$WF_{sample} = WF_{HOPG} - q \times (CPD_{sample} - CPD_{HOPG})$$

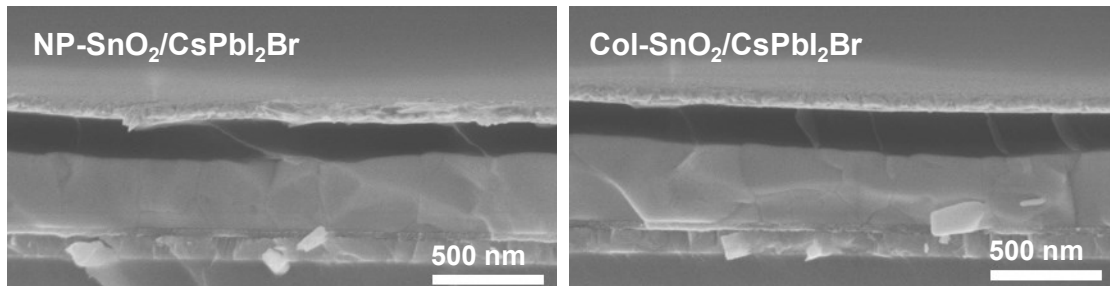


Figure S11. Cross-section SEM of the perovskite films deposited on NP-SnO₂ ETL and Col-SnO₂ ETL.

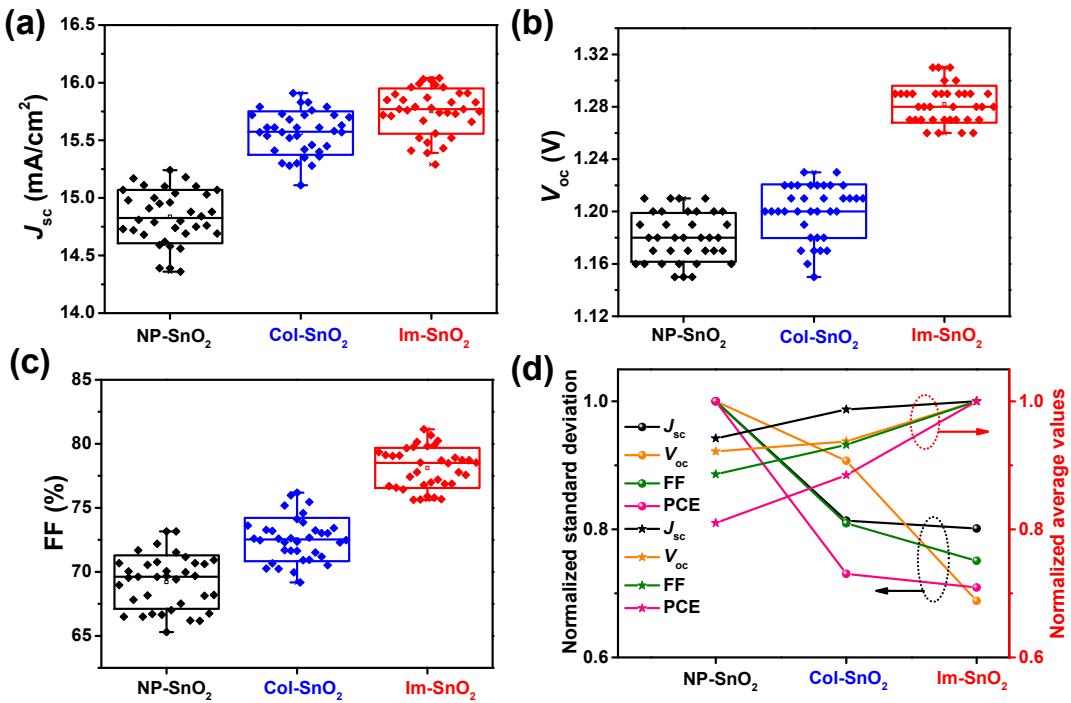


Figure S12. Device performance distribution of a) J_{sc} , b) V_{oc} , c) FF for 36 devices in one batch. d) The change trends of standard deviation and average values of different device parameters based on different SnO₂ ETLs. In order to show the amplitude of change for all these parameters in one figure clearly, all of these data are normalized.

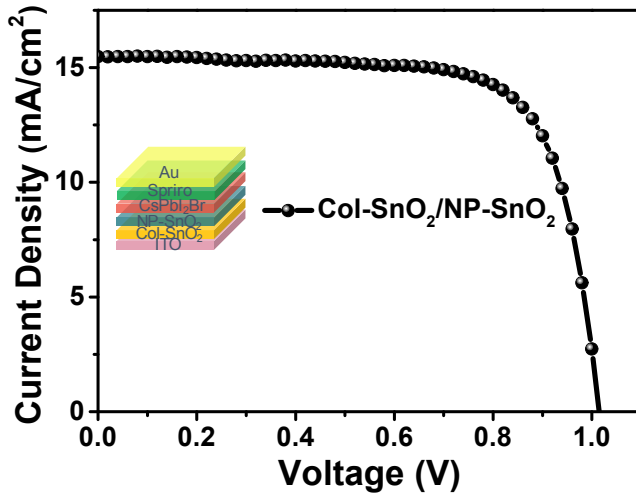


Figure S13. J - V characteristics of pero-SCs with a configuration of ITO/Col-SnO₂/NP-SnO₂/CsPbI₂Br/Spiro-OMeTAD/Au.

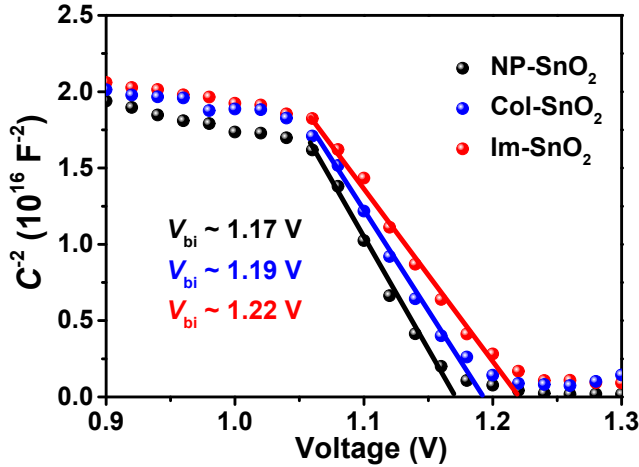


Figure S14. Mott-Schottky fitting to the capacitance-voltage (C^2 - V) plots of the CsPbI_2Br pero-SCs based on the different SnO_2 ETLs.

Table S1. Summary of Parameters and E_{loss} for High-efficiency All-inorganic Pero-SCs.

Device structure	E_g (eV)	J_{sc} (mA/cm²)	V_{oc} (V)	FF (%)	PCE (%)	E_{loss} (eV)	Ref.
FTO/TiO ₂ /CsPbI ₃ /PTAA/Au	1.69	18.95	1.059	74.9	15.07	0.631	[1]
FTO/c-TiO ₂ /m-TiO ₂ /CsPbI ₃ /Spiro-OMeTAD/Au	1.73	14.88	1.11	0.65	10.74	0.62	[2]
ITO/SnO ₂ /CsPbI ₃ /Spiro-OMeTAD/Au	1.73	18.41	1.08	79.32	15.71	0.65	[3]
FTO/TiO ₂ /CsPbI ₃ : Cl _{0.03} /PTAA/Au	1.73	19.58	1.084	75.7	16.07	0.646	[4]
ITO/PTAA/CsPb(I _{0.98} Cl _{0.02}) ₃ /PCBM/C ₆₀ /BCP/Cathode	1.72	14.9	1.08	70	11.4	0.64	[5]
FTO/c-TiO ₂ /m-TiO ₂ /CsPb _{0.875} Ca _{0.125} I ₃ /Spiro-OMeTAD/Au	1.77	16.37	0.84	66.91	9.20	0.93	[6]
FTO/TiO ₂ /PTABr-CsPbI ₃ /Spiro-OMeTAD/Ag	1.73	19.15	1.104	0.806	17.06	0.626	[7]
ITO/PTAA/CsPbI ₃ /C ₆₀ /BCP/Cu	1.76	17.8	0.96	76.0	12.5	0.80	[8]
FTO/TiO ₂ /CsPbI ₃ /Spiro-OMeTAD/Ag	1.68	20.49	1.101	81.1	18.30	0.579	[9]
ITO/SnO ₂ /CsPbI ₂ Br/CsBr/Spiro-OMeTAD/Au	1.90	16.72	1.271	77.18	16.37	0.629	[10]
FTO/TiO ₂ /CsPb _{0.9} Zn _{0.1} I ₂ Br/Spiro-OMeTAD/Ag	1.88	15.80	1.18	72.70	13.60	0.70	[11]
FTO/c-TiO ₂ /m-TiO ₂ /CsPb _{0.95} Eu _{0.05} I ₂ Br/Spiro-OMeTAD/Au	1.92	14.63	1.22	76.60	13.71	0.70	[12]
ITO/c-TiO ₂ /CsPbI ₂ Br/Spiro-OMeTAD/Au	1.90	16.79	1.23	77.81	16.07	0.67	[13]
FTO/TiO ₂ /CsPbBrI ₂ /PTAA/Au	1.91	12.93	1.19	80.50	12.39	0.72	[14]

FTO/NiOx/CsPbI ₂ Br/ZnO@C ₆₀ /Ag	1.92	15.20	1.14	77.00	13.30	0.78	[15]
ITO/SnO ₂ /PN4N/CsPbI ₂ Br/PDCBT/MoO ₃ /Ag	1.92	15.30	1.30	81.50	16.20	0.62	[16]
FTO/c-TiO ₂ /m-TiO ₂ /CsPbI ₂ Br/Spiro-OMeTAD/Au	1.90	13.98	1.17	74.00	12.00	0.73	[17]
FTO/TiO ₂ /CsPbI ₂ Br/Spiro-OMeTAD/Au	1.91	15.32	1.32	83.29	16.79	0.59	[18]
FTO/TiO ₂ /CsPbBr ₃ /Carbon	2.3	7.4	1.24	73	6.7	1.06	[19]
FTO/TiO ₂ /CsPbBr ₃ /Carbon	2.3	6.46	1.34	68.04	5.86	0.96	[20]
FTO/TiO ₂ /CsPbBr ₃ /Carbon	2.3	8.12	1.458	82.1	9.72	0.842	[21]
FTO/TiO ₂ /CsPbBr ₃ /Carbon	2.3	7.35	1.522	84.3	9.43	0.778	[22]
FTO/TiO ₂ /CsPbBr ₃ /P3HT:ZnPc/Carbon	2.3	7.652	1.578	83.06	10.03	0.722	[23]
FTO/TiO ₂ /SnO ₂ /CsPbBr ₃ /CuPc/Carbon	2.3	8.24	1.310	81.4	8.79	0.99	[24]
FTO/TiO ₂ /CQDs/CsPbBr ₃ /RPQDs/Carbon	2.3	7.33	1.470	76	8.2	0.83	[25]
ITO/ZnO/CsPbBr ₃ /Spiro-OMeTAD/Au	2.3	7.01	1.44	77.11	7.78	0.86	[26]
FTO/TiO ₂ /CsPb _{0.97} Sm _{0.03} Br ₃ /Carbon	2.3	7.48	1.594	85.1	10.14	0.706	[27]
FTO/TiO ₂ /CsPbIBr ₂ /Carbon	2.05	8.7	0.959	56	4.7	1.091	[28]
FTO/TiO ₂ /CsPbIBr ₂ /Carbon	2.05	9.11	1.142	63	6.55	0.908	[29]
FTO/c-TiO ₂ /CsPbIBr ₂ /Spiro-OMeTAD/Au	2.05	9.69	1.227	67.4	8.02	0.823	[30]
FTO/In ₂ S ₃ /CsPbIBr ₂ /Spiro-OMeTAD/Au	2.08	7.76	1.09	65.94	5.59	0.99	[31]
FTO/TiO ₂ /SmBr ₃ /CsPbIBr ₂ /PTAA	2.05	12.75	1.17	73	10.88	0.88	[32]
ITO/Im-SnO ₂ /CsPbI ₂ Br/Spiro-OMeTAD/Au	1.90	15.53	1.31	79.13	16.10	0.59	This Work

Table S2. Electron Mobilities of NP-SnO₂, Col-SnO₂ and Im-SnO₂ Calculated by SCLC Method.

Device Structure	Electron mobility (μ_e) (cm ² /V•s)
ITO/Al/NP-SnO ₂ /Al	1.54×10 ⁻⁴
ITO/Al/Col-SnO ₂ / Al	6.53×10 ⁻⁵
ITO/Al/Im-SnO ₂ /Al	2.14×10 ⁻⁴

Table S3. Calculated WF, E_v and E_c of the CsPbI₂Br and SnO₂ Fabricated by Different Methods.

Sample	E_{cutoff} (eV)	WF (eV)	E_v (eV)	E_g (eV)	E_c (eV)
NP-SnO ₂	16.85	4.37	-8.29	3.95	-4.34
Col-SnO ₂	16.97	4.25	-7.95	4.10	-3.85
Im-SnO ₂	16.89	4.33	-7.96	3.87	-4.09
CsPbI ₂ Br	17.25	3.97	-5.66	1.90	-3.76

Table S4. The Performance Parameters of Devices Based on Three Types of SnO₂ ETLs with Similar Thickness.

ETL	Thickness (nm)	V_{oc} (V)	J_{sc} (mA/cm ²)	FF (%)	PCE (%)
NP-SnO ₂	32.11	1.20	14.81	73.01	12.98
Col-SnO ₂	31.73	1.18	15.39	74.96	13.61
Im-SnO ₂	32.21	1.29	15.64	79.51	16.04

Table S5. Values for TRPL Characteristics of CsPbI₂Br Films Deposited on Different ETLs.

ETL	f_1 (%)	τ_1 (ns)	f_2 (%)	τ_2 (ns)
NP-SnO ₂	66.05	2.27	33.95	12.58
Col-SnO ₂	80.77	1.75	19.23	9.21
Im-SnO ₂	91.62	1.41	8.38	6.01

Table S6. Calculated Parameters for Saturation Current and Diode Ideality Factor of Devices Based on Different ETLs.

Device Structure	J_{sat} (mA/cm ²)	η
ITO/NP-SnO ₂ /CsPbI ₂ Br/Spiro/Au	2.57×10^{-9}	2.16
ITO/Col-SnO ₂ /CsPbI ₂ Br/Spiro/Au	4.06×10^{-6}	2.88
ITO/Im-SnO ₂ /CsPbI ₂ Br/Spiro/Au	1.21×10^{-11}	1.56

References

1. Wang, K.; Jin, Z.; Liang, L.; Bian, H.; Bai, D.; Wang, H.; Zhang, J.; Wang, Q.; Shengzhong, L., *Nat. commun.* **2018**, *9*, 4544.
2. Li, B.; Zhang, Y.; Fu, L.; Yu, T.; Zhou, S.; Zhang, L.; Yin, L., *Nat. Commun.* **2018**, *9*, 1076.
3. Wang, P.; Zhang, X.; Zhou, Y.; Jiang, Q.; Ye, Q.; Chu, Z.; Li, X.; Yang, X.; Yin, Z.; You, J., *Nat. Commun.* **2018**, *9*, 2225.
4. Wang, K.; Jin, Z.; Liang, L.; Bian, H.; Wang, H.; Feng, J.; Wang, Q.; Liu, S., *Nano Energy* **2019**, *58*, 175.
5. Wang, Q.; Zheng, X.; Deng, Y.; Zhao, J.; Chen, Z.; Huang, J., *Joule* **2017**, *1*, 371.
6. Zhao, H.; Xu, J.; Zhou, S.; Li, Z.; Zhang, B.; Xia, X.; Liu, X.; Dai, S.; Yao, J., *Adv. Funct. Mater.* **2019**, *29*, 1808986.
7. Wang, Y.; Zhang, T.; Kan, M.; Zhao, Y., *J Am. Chem. Soc.* **2018**, *140*, 12345.
8. Becker, P.; Márquez, J. A.; Just, J.; Al-Ashouri, A.; Hages, C.; Hempel, H.; Jošt, M.; Albrecht, S.; Frahm, R.; Unold, T., *Adv. Energy Mater.* **2019**, *9*, 1900555.
9. Wang, Y.; Dar, M. I.; Ono, L. K.; Zhang, T.; Kan, M.; Li, Y.; Zhang, L.; Wang, X.; Yang, Y.; Gao, X.; Qi, Y.; Gratzel, M.; Zhao, Y., *Science* **2019**, *365*, 591.
10. Zhang, Y.; Wu, C.; Wang, D.; Zhang, Z.; Qi, X.; Zhu, N.; Liu, G.; Li, X.; Hu, H.; Chen, Z.; Xiao, L.; Qu, B., *Sol. RRL* **2019**, *3*, 1900254.
11. Sun, H.; Zhang, J.; Gan, X.; Yu, L.; Yuan, H.; Shang, M.; Lu, C.; Hou, D.; Hu, Z.; Zhu, Y.; Han, L., *Adv. Energy Mater.* **2019**, *9*, 1900896.
12. Xiang, W.; Wang, Z.; Kubicki, D. J.; Tress, W.; Luo, J.; Prochowicz, D.; Akin, S.; Emsley, L.; Zhou, J.; Dietler, G.; Grätzel, M.; Hagfeldt, A., *Joule* **2018**, *3*, 205.
13. Chen, W.; Chen, H.; Xu, G.; Xue, R.; Wang, S.; Li, Y.; Li, Y., *Joule* **2019**, *3*, 191.
14. Zhang, J.; Bai, D.; Jin, Z.; Bian, H.; Wang, K.; Sun, J.; Wang, Q.; Liu, S. F., *Adv. Energy Mater.* **2018**, *8*, 1703246.
15. Liu, C.; Li, W.; Zhang, C.; Ma, Y.; Fan, J.; Mai, Y., *J. Am. Chem. Soc.* **2018**, *140*, 3825.
16. Tian, J.; Xue, Q.; Tang, X.; Chen, Y.; Li, N.; Hu, Z.; Shi, T.; Wang, X.; Huang, F.; Brabec, C. J.; Yip, H.-L.; Cao, Y., *Adv. Mater.* **2019**, *31*, 1901152.
17. Zeng, Z.; Zhang, J.; Gan, X.; Sun, H.; Shang, M.; Hou, D.; Lu, C.; Chen, R.; Zhu, Y.; Han, L., *Adv. Energy Mater.* **2018**, *8*, 1801050.
18. Han, Y.; Zhao, H.; Duan, C.; Yang, S.; Yang, Z.; Liu, Z.; Liu, S., *Adv. Funct. Mater.* **2020**, *30*, 1909972.
19. Liang, J.; Wang, C.; Wang, Y.; Xu, Z.; Lu, Z.; Ma, Y.; Zhu, H.; Hu, Y.; Xiao, C.; Yi, X.; Zhu, G.; Lv, H.; Ma, L.; Chen, T.; Tie, Z.; Jin, Z.; Liu, J., *J. Am. Chem. Soc.* **2016**, *138*, 15829.
20. Teng, P.; Han, X.; Li, J.; Xu, Y.; Kang, L.; Wang, Y.; Yang, Y.; Yu, T., *ACS Appl. Mater. Interfaces* **2018**, *10*, 9541.
21. Duan, J.; Zhao, Y.; He, B.; Tang, Q., *Angew. Chem. Int. Ed.* **2018**, *57*, 3787.
22. Duan, J.; Hu, T.; Zhao, Y.; He, B.; Tang, Q., *Angew. Chem. Int. Ed.* **2018**, *57*, 5746.
23. Liu, Y.; He, B.; Duan, J.; Zhao, Y.; Ding, Y.; Tang, M.; Chen, H.; Tang, Q., *J. Mater. Chem. A* **2019**, *7*, 12635.
24. Liu, X.; Tan, X.; Liu, Z.; Ye, H.; Sun, B.; Shi, T.; Tang, Z.; Liao, G., *Nano Energy* **2019**, *56*, 184.
25. Liao, G.; Duan, J.; Zhao, Y.; Tang, Q., *Sol. Energy* **2018**, *171*, 279.
26. Chen, W.; Zhang, J.; Xu, G.; Xue, R.; Li, Y.; Zhou, Y.; Hou, J.; Li, Y., *Adv. Mater.* **2018**, *30*, e1800855.
27. Duan, J.; Zhao, Y.; Yang, X.; Wang, Y.; He, B.; Tang, Q., *Adv. Energy Mater.* **2018**, *8*, 1802346.
28. Ma, Q.; Huang, S.; Wen, X.; Green, M. A.; Ho-Baillie, A. W. Y., *Adv. Energy Mater.* **2016**, *6*, 1502202.
29. Zhu, W.; Zhang, Q.; Chen, D.; Zhang, Z.; Lin, Z.; Chang, J.; Zhang, J.; Zhang, C.; Hao, Y., *Adv. Energy Mater.* **2018**, *8*, 1802080.
30. Li, W.; Rothmann, M. U.; Liu, A.; Wang, Z.; Zhang, Y.; Pascoe, A. R.; Lu, J.; Jiang, L.; Chen, Y.; Huang, F.; Peng,

- Y.; Bao, Q.; Etheridge, J.; Bach, U.; Cheng, Y.-B., *Adv. Energy Mater.* **2017**, *7*, 1700946.
31. Yang, B.; Wang, M.; Hu, X.; Zhou, T.; Zang, Z., *Nano Energy* **2019**, *57*, 718.
32. Tan, H.; Jain, A.; Voznyy, O.; Lan, X.; Garcia de Arquer, F. P.; Fan, J. Z.; Quintero-Bermudez, R.; Yuan, M.; Zhang, B.; Zhao, Y.; Fan, F.; Li, P.; Quan, L. N.; Zhao, Y.; Lu, Z. H.; Yang, Z.; Hoogland, S.; Sargent, E. H., *Science* **2017**, *355*, 722.